Research paper

Selective adsorption of BTEX on calixarene-based molecular coordination network determined by ^{13}C NMR spectroscopy

Allana Christina de Oliveira Frós[a], Maria Alaide de Oliveira[a], Antonia Alice Macêdo Soares[a], Fernando Hallwass[a], Jaroslaw Chojnacki[b], Bráulio Silva Barros[c,*], Severino Alves Júnior[a], Joanna Kulesza[a,*]

[a] *Universidade Federal de Pernambuco, Departamento de Química Fundamental, Av. Prof. Moraes Rego, 1235 –Cidade Universitária, 50670-901 Recife, PE, Brazil*
[b] *Department of Inorganic Chemistry, Chemical Faculty, Gdansk University of Technology, G. Narutowicza 11/12 Street, 80-233 Gdansk, Poland*
[c] *Universidade Federal de Pernambuco, Departamento de Engenharia Mecânica, Av. Prof. Moraes Rego, 1235 – Cidade Universitária, 50670-901 Recife, PE, Brazil*

A B S T R A C T

Benzene, toluene, ethylbenzene, and xylenes (BTEX), a class of volatile organic compounds, are harmful pollutants but also very important precursors in organic industrial chemistry. Among different approaches used for the BTEX treatment, the adsorption technology has been recognized as an efficient approach because it allows to recover and reuse both adsorbent and adsorbate. However, the selective adsorption of the components is the key factor for the efficiency of the process. With this view, calixarene-based materials are very promising due to the unique cavity-like structure of the ligand. An unprecedented coordination network based on calixarene of an interesting nanosheet-like morphology was prepared *via a* solvothermal layer method. This material showed selectivity for non-polar molecules with remarkable uptake of benzene (38.33 mmol/g). In addition, a simple and useful method of BTEX quantification, through ^{13}C NMR spectroscopy, is reported here for the first time.

1. Introduction

BTEX (benzene, toluene, ethylbenzene, and xylenes) belong to the class of volatile organic compounds (VOCs) and are known as harmful pollutants due to their toxic, mutagenic and carcinogenic nature. On the other hand, these compounds are very important precursors in organic industrial chemistry and are widely used in the manufacture of solvents, paints and paint removers, polymers, glues, and electronics.

Numerous BTEX treatment technologies have been developed, which can be divided into destruction methods and recovery methods [1]. Although effective, most of the destruction methods, such as oxidation, incineration or photocatalysis, requires enormous amounts of energy, and produce some toxic byproducts. Compared to the destructive methods, the recovery methods which include adsorption, condensation, and membrane separation, are environmentally friendly and more economic. However, the reuse of the recovered compounds must be preceded by the effective separation of the components. This is a difficult task since these compounds possess very similar physicochemical properties which hinder their separation by methods such as simple or fractional distillation. The efficient separation of xylenes (*o*-, *m*-, *p*-xylenes) from ethylbenzene is especially challenging due to their very close boiling points [1].

Among the recovery methods, the adsorption technology has been recognized as an efficient approach because it allows to recover and reuse both adsorbent and adsorbate. Porous adsorbents such as carbonaceous materials (activated carbon, biochar, ordered mesoporous carbon, carbon nanotubes, graphene, and its derivatives) have been widely used for BTEX adsorption [2]. For example, recently, Saha et al. have tested the lignin-derived activated carbon and showed the adsorption amounts of benzene, toluene or xylene were very similar (up to 6.5 mmol/g in the vapor phase), and therefore, the adsorbent could not be used to separate those components from each other [3]. Such lack of selectivity is mainly caused by irregular shape and size of particles which is common for most of the activated and porous carbons [2]. Among other tested materials, zeolites exhibit low adsorption capacity caused by poor interactions of BTEX with the inorganic matrix. For instance, Vellingiri et al. showed that 4A Zeolite could adsorb only 0.33 mmol/g of toluene [4].

In this scenario, coordination polymers (CPs) and MOFs (Metal-Organic Frameworks), have emerged as promising materials for selective adsorption processes, and are now among the most studied platforms for BTEX treatment, owing to their structural diversity, intriguing

---

topologies, and adjustable pore size [4]. Zhao et al. have shown that HKUST-1 can adsorb 9.42 mmol/g of benzene at 318 K and 24 mbar and 8.32 mmol/g in the competitive adsorption with water at 1.0 mbar [5]. Chromium-based metal-organic framework MIL-101 showed high adsorption capacity of benzene (16.7 mmol/g [6] and 16.4 mmol/g [7]). Yang et al. have also tested the affinity of MIL-101(Cr) towards other BTEX components and found the efficient adsorption for toluene (11.9 mmol), ethylbenzene (10.4 mmol), and *p*-xylene (10.1 mmol). The material also adsorbed significant amounts of *m*-xylene (6.8 mmol) and *o*-xylene (7.1 mmol) [7]. The adsorption capacity of benzene, toluene, ethylbenzene and xylene components in MOF-177 has been investigated. The material showed an adsorption capacity of 10.24 and 6.35 mmol/g, for benzene and toluene, respectively. Since the pores in the structure of MOF-177 are large enough to accommodate any BTEX component, ethylbenzene and xylene isomers were also adsorbed in similar quantities (about 2.5 mmol/g each of the component), reflecting the low selectivity of the material [8].

Most of the studies report vapor phase adsorption, while the adsorption experiments in the liquid phase are rare and are mostly focused on the qualitative determination of BTEX uptake [9,10]. It is well known that adsorptive properties of metal-organic materials essentially depend on the choice of the organic ligand. Calixarenes represent a class of macrocyclic ligands commonly known as versatile host compounds able to form stable complexes of the host-guest type with metal ions or neutral molecules such as BTEX components [11–13], owing to the π-π and/or π-CH₃ interactions between phenolic rings of a calixarene and a neutral hydrocarbon molecule. More recently, calixarenes have been successfully used as secondary building units in a self-assembly process of 1D-3D coordination polymers [14]. The construction of coordination polymers based on calixarenes has been mainly focused on upper-rim sulfonate and in less extend carboxylate derivatives. Only a few articles have been published about coordination polymers based on calixarenes appended with carboxylate groups on lower rim [15–17]. Most of these works are devoted to the structure of such materials, and little has been reported on their applications. Coordination networks based on calixarenes may find use as efficient platforms for the selective adsorption and separation of BTEX.

With this view, a novel molecular coordination network containing *p-tert*-butyl-calix[4]arene tetracarboxylate calix-TAA and Zn^{2+} ions was tested in the competitive adsorption of BTEX. According to our best knowledge, this is the first example of the application of calixarene-based material for BTEX adsorption. We also communicate here for the first time, a very useful and simple method of ¹³C qNMR (carbon-13 quantitative nuclear magnetic resonance spectroscopy) [18–20] for the analysis and quantification of hydrocarbon compounds adsorbed in MOFs.

2. Experimental

2.1. Materials

All reagents and solvents were used as received without further purification. *p-tert*-Butyl-calix[4]arene and ethyl bromoacetate were acquired from Sigma Aldrich. K_2CO_3, KOH, $MgSO_4$, Zn $(CH_3COO)_2 \cdot 2H_2O$ (ZnAc₂·2H₂O); and solvents: dimethylformamide (DMF), acetone, dichloromethane (CH_2Cl_2), chloroform ($CHCl_3$), methanol (MeOH), ethanol (EtOH) and hydrochloric acid (HCl) were purchased from Vetec. $CDCl_3$ (99.9% deuterated) and 1,4-dioxane (99.0%) for NMR analyses were purchased from Sigma Aldrich. For the adsorption tests, the solvents benzene (C_6H_6), toluene (C_7H_8) and xylene (C_8H_{10}) were purchased from Vetec.

The ligand *p-tert*-butyl-25,26,27,28-tetrakis(carboxymethoxy)calix [4]arene, calix-TAA was prepared in two steps according to the procedure described in the literature [21,22].

2.2. Preparation and characterization of the adsorbent

Calixarene-based coordination network calix-TAA-Zn was obtained by the solvothermal method as follows: an aqueous solution of Zn $(Ac)_2 \cdot 2H_2O$ (0.0044 g, 0.02 mmol) (5 mL) was placed in a thick-walled glass vial, and then a layer of DMF (5 mL) was carefully placed on top of the solution. Subsequently, 0.053 g (0.06 mmol) of the ligand calix-TAA were dissolved in DMF (5 mL), and the solution was placed as the last layer in the reaction vial. The reaction was performed at 90 °C for four days. The resulting white sheet-like crystals (insoluble in any organic solvent or water) were filtered off, washed with DMF and ethanol and dried in an oven at 60 °C for 2 h.

The samples (calix-TAA and calix-TAA-Zn) were characterized by Fourier Transform Infrared Spectroscopy (FTIR) and Scanning Electron Microscopy (SEM). ATR-FTIR experiments were carried out on a Bruker Vertex 70/v spectrometer at the range of 4000–700 cm⁻¹. Morphological analysis of powders was performed in a Shimadzu SS-550 Microscope equipment with 15 kV acceleration.

2.3. NMR measurements

¹H and ¹³C NMR spectra were acquired in an NMR spectrometer Agilent 400 MHz at 298 K in 5 mm NMR tube. $CDCl_3$ was used as a solvent and internal chemical shift reference. ¹³C longitudinal relaxation times (T_1) were measured using standard Inversion-Recovery pulse sequence. qNMR spectra were acquired with a spectral width of 23.6 kHz, the acquisition time of 1.39 s, 32 k memory data points, interpulse delay of 50 s (5 × highest T_1 value, see SI), excitation pulse of 45° and 16 transients. To eliminate NOE effects, the decoupler was gated on only during acquisition. The signal integrations were computed according to the GSD protocol [23] using Mnova 11.04 software.

2.4. Adsorption experiments

The adsorption capacity of calix-TAA-Zn was evaluated in competitive adsorption experiments in a liquid phase at room temperature. For comparison, the same tests were repeated using the pure ligand calix-TAA as the adsorbent.

Before the experiments, the adsorbents (calix-TAA and calix-TAA-Zn) were dried overnight at 120 °C. 30 mg of the adsorbent were put in contact without stirring with the BTEX solution of the known composition and concentration for 2 h. After this time, the supernatant solution of BTEX was withdrawn immediately and placed in a 5 mm NMR tube, 300 μL of $CDCl_3$ were added, and ¹³C qNMR spectrum was acquired. Four different BTEX solution systems were tested: A (0.5 mL of xylene); B (0.5 mL of xylene and 0.5 mL of toluene); C (0.5 mL of xylene and 0.5 mL of benzene); and D (0.5 mL of xylene, 0.5 mL of benzene, and 0.5 mL of toluene). In parallel, blank experiments were also conducted by using BTEX solutions without adsorbent for all systems and were analyzed under the same conditions as the adsorption solutions.

The quantification of the BTEX adsorption was carried out indirectly by determining the quantity of each component before the adsorption (blank experiment without adsorbent, Spectrum 1) and after the adsorption process (adsorption experiment, Spectrum 2). The adsorbed amount is related to the difference between the quantities of the components before and after adsorption, measuring by the integrals area of both spectra.

The number of mols from a component x (n_x) present in a system can be calculated using Eq. (1) [18,19,24]:

$$n_x = \frac{I_x}{I_y}\frac{N_y}{N_x}n_y \tag{1}$$

where I_x corresponds to the integral from one signal of component x, and N_x is the number of the carbons in the molecule of x present in this signal. In the same way, I_y is integral from one signal of the component

y, which has a known concentration in the solution (used as reference for the quantification), n_y is the number of mols of component y, and N_y is the number of the carbons in the molecule of y present in this signal (see SI). Consequently, the number of mols adsorbed ($n_{adsorbed}$) is the difference of the number of mols of the BTEX in Spectrum 1 (n_{x1}) and Spectrum 2 (n_{x2}) given by:

$$n_{adsorbed} = n_{x_1} - n_{x_2} \qquad (2)$$

$$n_{adsorbed} = \frac{I_{x_1}}{I_y}\frac{N_y}{N_x}n_y - \frac{I_{x_2}}{I_y}\frac{N_y}{N_x}n_y \qquad (3)$$

$$n_{adsorbed} = n_y \frac{N_y}{N_x}\left(\frac{I_{x_1}}{I_y} - \frac{I_{x_2}}{I_y} \right) \qquad (4)$$

Considering $I_{x_1} - I_{x_2}$ as ΔI_x, we have:

$$n_{adsorbed} = \frac{\Delta I_x}{I_y}\frac{N_y}{N_x}n_y \qquad (5)$$

Eq. (5) was used in this work to quantify all the systems studied.

Initially, 1,4-dioxane (100 μL) was used as a reference for quantification in all studied systems to verify the adsorption uptake of each component from the solution (A, B, C or D). Because ethylbenzene, present in the xylene, was not adsorbed from any of the systems, it was then used as a reference for the quantification.

All adsorption experiments were done in triplicate, and the integral area corresponds to the average of the integrals measured ten times.

3. Results and discussion

3.1. Sample characterization

Fig. 1 shows the IR spectra of the obtained material calix-TAA-Zn and pure ligand. The bands in the region of 2867–2955 cm^{-1} and at 1478 cm^{-1} correspond to the alkyl C—H and aromatic C=C stretching, respectively. These bands are also observed in the spectrum of the pure ligand, indicating the presence of the calixarene moiety in the structure of calix-TAA-Zn. The intense band at 1743 cm^{-1} observed in the IR spectrum of the pure ligand corresponds to the ν (C=O) stretching of COOH groups. This band is also visible (although less intense) in the IR spectrum of calix-TAA-Zn, indicating the presence of at least one protonated carboxylic acid group in the structure. The IR spectrum of calix-TAA-Zn presents the new intense broad band (possibly composed of more than one overlapped band) centered at 1593 cm^{-1} related to the asymmetric stretching of the deprotonated COO$^-$ groups. The presence of this band suggests the formation of the zinc-carboxylate coordination bonds.
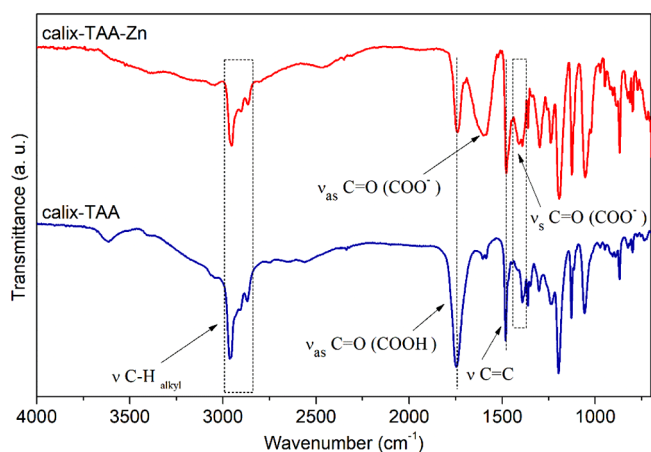

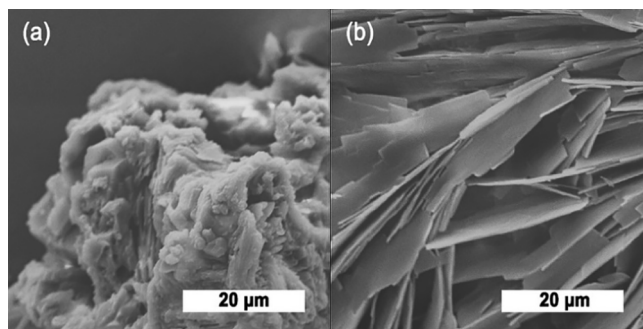**Fig. 1.** FT-IR spectra of the pure ligand calix-TAA and the prepared sample calix-TAA-Zn.

Fig. 2. SEM images of (a) calix-TAA and (b) calix-TAA-Zn.

Therefore, we assume that one of the carboxylic acid groups remains protonated, whereas the other three groups are deprotonated and coordinated to the metal center. Moreover, in the region of symmetric stretching of COO$^-$ groups, two bands at 1410 and 1388 cm^{-1} are visible, instead of one band as observed for the pure ligand. The difference between wavenumbers ($\Delta\bar{\upsilon}$) of the stretching, asymmetric and symmetric of COO$^-$ groups provides useful information about coordination modes of carboxylate groups [25]. The values of $\Delta\bar{\upsilon}$ around 183 and 205 cm^{-1} indicate the presence of mono-, bi-dentate and/or chelate coordination modes in the structure of calix-TAA-Zn. The proposed structure of calix-TAA-Zn is presented in Figs. S1 and S2.

The prepared material calix-TAA-Zn presents an interesting regular nanosheet-like morphology, whereas the pure ligand shows agglomerates of irregular shape particles, as shown on scanning electron micrographs (Fig. 2).

3.2. Xylene quantification

The xylene used in this work consisted of the mixture of four compounds, namely: ortho-xylene (oX), meta-xylene (mX), para-xylene (pX) and ethylbenzene (EB), as verified by NMR spectroscopy (see Figs. S3–S5 and Table S3). ^{1}H NMR spectrum of xylene presents a complex pattern with overlapping signals in the aromatic and methyl groups regions, inappropriate for quantification. However, ^{13}C NMR spectrum shows a better signal separation, and the region between 16.4 and 22.0 ppm, corresponding to the methyl groups, can be used for the quantification of the xylene components following the protocols for quantitative analyses described in the literature [24] (see details in SI). The NMR data for the quantification of xylene are presented in Table 1. Based on ^{13}C NMR spectra, it was found that the composition of xylene was as follow: EB (71.1%), oX (2.7%), mX (17.7%) and pX (8.5%).

3.3. BTEX adsorption

The liquid-phase adsorption of BTEX in calix-TAA-Zn and calix-TAA at ambient conditions was studied in four different systems: xylene (A); xylene and toluene (1:1) (B); xylene and benzene (1:1) (C); xylene, toluene and benzene (1:1:1) (D). Fig. 3 presents the ^{13}C qNMR spectra before (Spectrum 1) and after adsorption (Spectrum 2) on calix-TAA-Zn

Table 1
NMR data for the quantification of xylene.

Compound	Integration area[*]	Percentage (%)	Quantity[**]	
			(mg)	(mmol)
Ethylbenzene (EB)	100.0	71.1	307.8	2.90
o-xylene (oX)	7.6	2.7	11.8	0.11
m-xylene (mX)	49.6	17.7	76.6	0.72
p-xylene (pX)	24.0	8.5	36.8	0.35

[*] Maximum error of 1%.
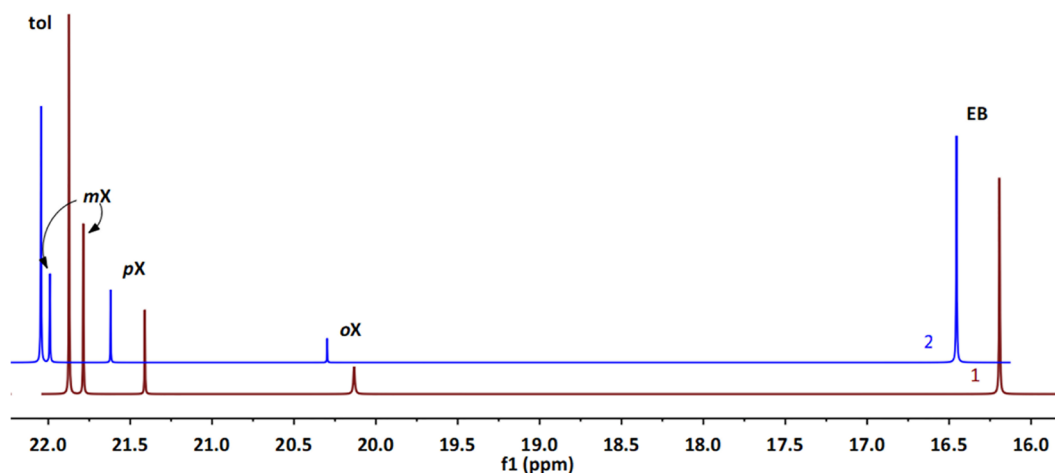[**] Considering the volume of the sample 0.5 mL.

Fig. 3. Expansion of ^{13}C NMR spectra of the methyl groups region of the system B: (1) before and (2) after the adsorption process on calix-TAA-Zn. Signals are marked for clarity, EB δ = 16.3 ppm; oX δ = 20.2 ppm; pX δ = 21.4 ppm; mX δ = 21.5 ppm; toluene δ = 21.8 ppm.

for system B, as an example. The representative spectra and the calculations of the quantification analyses for all systems are detailed in SI (Figs. S6–S10, Tables S4–S11).

The percentage of BTEX adsorption on calix-TAA-Zn and the free ligand calix-TAA are shown in Fig. 4. The coordination network calix-TAA-Zn exhibits an excellent benzene uptake of 1.15 mmol/30 mg (38.33 mmol/g) corresponding to 20.4% of the adsorption for the system C containing ethylbenzene and xylene isomers. In the absence of benzene, calix-TAA-Zn shows a preference for p-xylene with 42.6 and 14.0% of the adsorption for systems A and B, respectively. Although the initial quantity of toluene was much higher than of p-xylene (4.7 mmol vs. 0.35 mmol), the prepared material showed selectivity for p-xylene with the percentage adsorption almost two times higher than for toluene (system B). In the competitive adsorption with toluene and benzene (system D), calix-TAA-Zn adsorbed almost equal quantities of benzene and toluene with the adsorption percentages of 8.9 and 8.1% for toluene and benzene, respectively. The adsorption of toluene is very

similar for the studied mixtures with 8.5 and 8.9%, for system B and D, respectively.

Interestingly, ethylbenzene (which was the most abundant in the xylene) was not adsorbed on calix-TAA-Zn from any of the systems. This fact may be explained by the much larger size of the ethylbenzene molecule (EB 6.625 Å × 5.285 Å × 9.361 Å) than any other BTEX component. Additionally, the lateral chain of ethylbenzene can cause a steric hindrance in the surface interactions with calix-TAA-Zn.

Although the molecular dimensions of xylene isomers are relatively similar (oX: 7.269 Å × 3.834 Å × 7.826 Å; mX: 8.994 Å × 3.949 Å × 7.315 Å; pX: 6.618 Å × 3.810 Å × 9.146 Å), the amount of each isomer adsorbed on the prepared material varied significantly. This fact may be associated with the steric hindrance resulted from the molecular shape, more specifically, the position of the methyl groups in the molecules. It is worth noting that the adsorption affinity of calix-TAA-Zn for C_8H_{10} molecules always follows the same order for all systems studied: p-xylene > m-xylene > o-xylene > ethylbenzene. Among
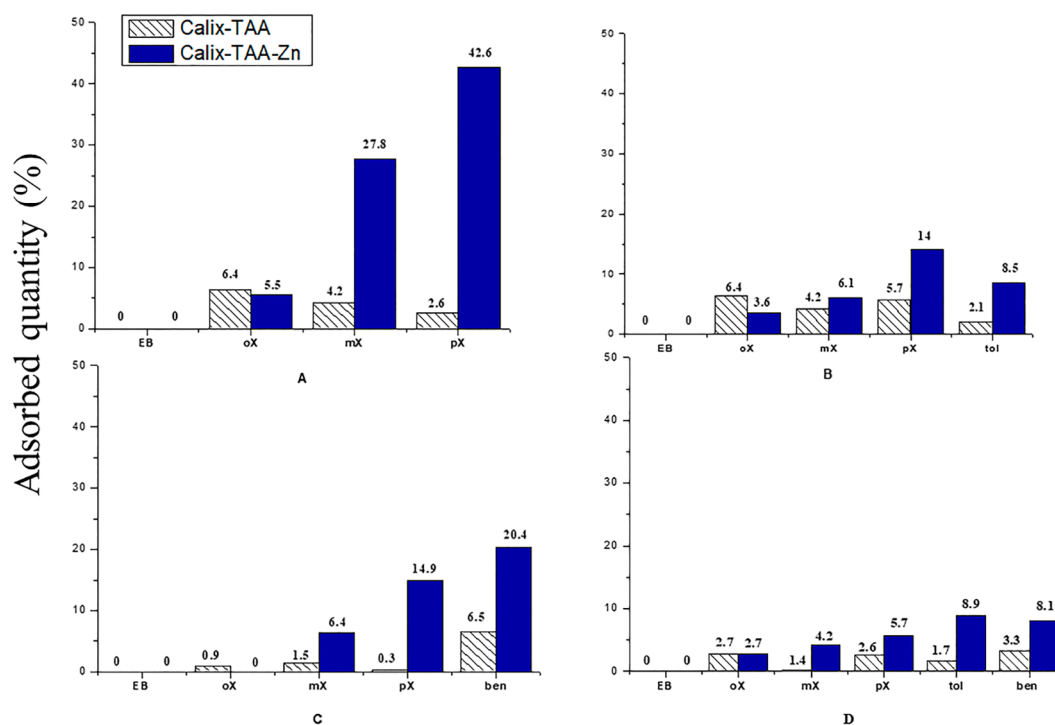

Fig. 4. Comparison of the quantity of the adsorbed BTEX components in different systems on calix-TAA-Zn and calix-TAA in mmol/g.

xylene isomers, *o*-xylene was adsorbed in the smallest quantities in all cases (< 6.5%). The adsorption of *o*-xylene decreases even more (or completely) in the presence of benzene in the solution.

The affinity order for BTEX can be partially explained based on the polarity of the molecules. The apolarity order for the studied molecules is: *p*-xylene (μ = 0 D) = benzene (μ = 0 D) > *m*-xylene (μ = 0.30 D) > ethylbenzene (μ = 0.36 D) > toluene (μ = 0.43 D) > *o*-xylene (μ = 0.51 D). Therefore, we can conclude that calix-TAA-Zn demonstrates the preference for non-polar molecules (*p*-xylene and benzene), what is in agreement with the proposed hydrophobic structure of calix-TAA-Zn (see Fig. S1). Probably, in the structure of calix-TAA-Zn, the cavities of the calixarenes are in front to each other, which may exclude the encapsulation of molecules within the cavities. On the other hand, there are only weak interactions between the hydrophobic lamellas, and in the host crystals, some voids may be found between the layers (see Fig. S2). Therefore, with little expense of energy, additional small molecules can be adapted by a kind of intercalation, resulting in small elongation of the unit cell. It appears the adsorption affinity of calix-TAA-Zn is governed by the combination of two factors: i) polarity of molecules and ii) steric and size complementarity between the molecules and interlamellar voids present in the structure of calix-TAA-Zn.

Compared to the coordination network calix-TAA-Zn, the free ligand calix-TAA is a poor adsorbent with the significant adsorption only of *o*-xylene (6.4%, system A and B) and benzene (6.5%, system C). The adsorption percentage of other BTEX components is very low (< 6%). No clear selectivity may be observed in the case of the pure ligand calix-TAA, although the highest uptake for benzene from the mixture of all BTEX components (system D), may suggest the preference for non-polar molecules. The quantity of benzene adsorbed onto calix-TAA, however, is more than two times lower than for calix-TAA-Zn.

To compare the adsorption capacity of BTEX components by the synthesized materials with other adsorbents known from the literature, the values are presented in mmol per 1 g of the adsorbent. The excellent amount of benzene adsorbed on calix-TAA-Zn (38.33 mmol/g, system C) is much higher than for reported MOFs like MOF-177 (10.24 g/mol) [8], MIL-101(Cr), 16.7 mmol/g [6] and 16.4 mmol/g [7], and other adsorbents, such as activated carbon (6.5 mmol/g) [4]. The uptake of toluene by calix-TAA-Zn (13.33 mmol/g) is higher than by common MOFs such as UIO-66 (1.80 mmol/g) [4], UIO-NH$_2$ (2.74 mmol/g) [4], ZIF-67 (2.43 mmol/g) [4] , MOF-199 (1.73 mmol/g) [4], MIL-101(Fe) (1.07 mmol/g) [4], MOF-5 (0.36 mmol/g) [4], HKUST-1 (9.42 mmol/g) [5], MIL-101(Cr) (11.9 mmol/g) [7], MOF-177 (6.35 mmol/g) [8], zeolites (4A Zeolite, 0.33 mol/g) [4], and activated carbon (6.5 mmol/g) [3].

The improved capacity of benzene or toluene adsorption may be associated with the unique characteristics of calixarene ligand present in the structure of calix-TAA-Zn. The shape of the aromatic cavity of calixarenes enhances the adsorption capacity through π–π and CH$_3$–π interactions which are stronger than C-π and O-π interactions between aromatic BTEX molecules and carbon materials or zeolites. Even the free ligand calix-TAA, in some cases, is more efficient in the adsorption of toluene (3.33 mmol/g, system B) or benzene (12.2 mmol/g, system C) than other reported adsorbents which affirm the efficiency of the calixarene cavity in the host-guest complexation.

4. Conclusions

In summary, a novel calixarene-based molecular coordination network calix-TAA-Zn of an interesting nanosheet-like morphology was successfully synthesized *via* a solvothermal layer method. Calix-TAA-Zn showed a preference for non-polar molecules with the remarkable benzene adsorption from the liquid phase containing the mixture of BTEX components (toluene, benzene, ethylbenzene, and xylenes). Moreover, to the best of our knowledge, calix-TAA-Zn is the first example of an organic-inorganic molecular material with such a good separation of xylene isomers from ethylbenzene. The use of calixarene-

based materials is a promising strategy that could reach both high adsorption capacity and separation selectivity from the aromatic mixture. Further studies will include the optimization of adsorption capacity of calix-TAA-Zn and other calixarene-based materials. We demonstrated that ^{13}C NMR spectroscopy is a useful technique for the quantification of BTEX components and may be helpful for the determination of other C-based molecules.

Appendix A. Supplementary data

Supplementary data to this article can be found online at https://doi.org/10.1016/j.ica.2019.04.031.

References

[1] Y. Zhou, J. Wu, E.W. Lemmon, Thermodynamic properties of o-Xylene, m-Xylene, p-Xylene, and Ethylbenzene, J. Phys. Chem. Ref. Data 41 (2012), https://doi.org/10.1063/1.3703506.

[2] X. Zhang, B. Gao, A.E. Creamer, C. Cao, Y. Li, Adsorption of VOCs onto engineered carbon materials: a review, J. Hazard. Mater. 338 (2017) 102–123, https://doi.org/10.1016/j.jhazmat.2017.05.013.

[3] D. Saha, N. Mirando, A. Levchenko, Liquid and vapor phase adsorption of BTX in lignin derived activated carbon: equilibrium and kinetics study, J. Clean. Prod. 182 (2018) 372–378, https://doi.org/10.1016/j.jclepro.2018.02.076.

[4] K. Vellingiri, P. Kumar, A. Deep, K.H. Kim, Metal-organic frameworks for the adsorption of gaseous toluene under ambient temperature and pressure, Chem. Eng. J. 307 (2017) 1116–1126, https://doi.org/10.1016/j.cej.2016.09.012.

[5] Z. Zhao, S. Wang, S. Yang, X. Li, J. Li, Z. Li, Competitive adsorption and selectivity of benzene and water vapor on the microporous metal organic frameworks (HKUST-1), Chem. Eng. J. 259 (2015) 79–89, https://doi.org/10.1016/j.cej.2014.08.012.

[6] Z.L.Z. Zhao, X. Li, S. Huang, Q. Xia, Adsorption and diffusion of benzene on chromium-based metal organic framework MIL-101 synthesized by microwave irradiation, Ind. Eng. Chem. Res. 50 (2011) 2254–2261, https://doi.org/10.1021/ie101414n.

[7] K. Yang, Q. Sun, F. Xue, D. Lin, Adsorption of volatile organic compounds by metal – organic frameworks MIL-101: Influence of molecular size and shape, J. Hazard. Mater. 195 (2011) 124–131, https://doi.org/10.1016/j.jhazmat.2011.08.020.

[8] K. Yang, F. Xue, Q. Sun, R. Yue, D. Lin, Journal of environmental chemical engineering adsorption of volatile organic compounds by metal-organic frameworks MOF-177, J. Environ. Chem. Eng. 1 (2013) 713–718, https://doi.org/10.1016/j.jece.2013.07.005.

[9] J. Cheng, P. Wang, J.-P. Ma, Q. Liu, Y. Dong, A nanoporous Ag(< scp > i < /scp >)-MOF showing unique selective adsorption of benzene among its organic analogues, Chem. Commun. 50 (2014) 13672–13675, https://doi.org/10.1039/C4CC03204G.

[10] F. Yang, Q.-K. Liu, J.-P. Ma, Y.-A. Li, K.-X. Wang, Y.-B. Dong, Reversible adsorption and separation of chlorocarbons and BTEX based on Cu(< scp > ii < /scp >)-metal organic framework, CrystEngComm 17 (2015) 4102–4109, https://doi.org/10.1039/C5CE00547G.

[11] S. Kumar, S. Chawla, M.C. Zou, Calixarenes based materials for gas sensing applications: a review, J. Incl. Phenom. Macrocycl. Chem. 88 (2017) 129–158, https://doi.org/10.1007/s10847-017-0728-2.

[12] K.S. Choi, Sung-Seen Nam, The characterization of toluene-p-t-butylcalix[4]arene complexes using thermal analyses, Bull. Korean Chem. Soc. 20 (1999) 595–596.

[13] B. Lemli, J. Peles, L. Kollár, G. Nagy, S. Kunsági-Máté, K.C.N. Sung-Seen Choi, The rate of host-guest complex derivatives formation towards neutral aromatic guests, Supramol. Chem. 18 (2006) 251–256, https://doi.org/10.1080/10610270500450416.

[14] A. Ovsyannikov, S. Soloviева, I. Antipin, S. Ferlay, Coordination polymers based on calixarene derivatives: structures and properties, Coord. Chem. Rev. 352 (2017) 151–186, https://doi.org/10.1016/j.ccr.2017.09.004.

[15] C. Redshaw, O. Rowe, M.R.J. Elsegood, L. Horsburgh, S.J. Teat, Pillared two-dimensional metal-organic frameworks based on a lower-rim acid appended calix[4]arene, Cryst. Growth Des. 14 (2014) 270–277, https://doi.org/10.1021/cg4014703.

[16] C. Redshaw, O. Rowe, D.L. Hughes, A-M. Fuller, I.A. Ibarra, S.M. Humphrey, New structural motifs in lithium and zinc calix[4]arene chemistry, Dalt. Trans. 42 (2013) 1983–1986, https://doi.org/10.1039/c2dt32986g.

[17] R.S. Viana, C.A.F. Oliveira, J. Chojnacki, B.S. Barros, S. Alves-Jr, J. Kulesza,

Structural and spectroscopic investigation of new luminescent hybrid materials based on calix[4]arene-tetracarboxylate and Ln3 + ions (Ln = Gd, Tb or Eu), J. Solid State Chem. 251 (2017) 26–32, https://doi.org/10.1016/j.jssc.2017.04.002.

[18] F. Malz, H. Jancke, Validation of quantitative NMR, J. Pharm. Biomed. Anal. 38 (2005) 813–823, https://doi.org/10.1016/j.jpba.2005.01.043.

[19] J.N. Shoolery, Some quantitative applications of 13C NMR spectroscopy, Prog. Nucl. Magn. Reson. Spectrosc. 11 (1977) 79–93, https://doi.org/10.1016/0079-6565(77)80003-4.

[20] U. Holzgrabe, Quantitative NMR spectroscopy in pharmaceutical R&D, EMagRes 4 (2015) 45–56, https://doi.org/10.1002/9780470034590.emrstm1399.

[21] F. Arnaud-Neu, E. Marques, M.J. Schwing-Weill, E.M. Collins, M. Deasy, M.A. McKervey, E.M. Seward, G. Ferguson, B. Kaitner, A.J. Lough, B.L. Ruhl, S.J. Harris, Synthesis, X-ray crystal structures, and cation-binding properties of alkyl calixaryl esters and ketones, a new family of macrocyclic molecular receptors, J. Am. Chem. Soc. 111 (1989) 8681–8691, https://doi.org/10.1021/ja00205a018.

[22] F. Arnaud-Neu, G. Barrett, S. Cremin, M. Deasy, G. Ferguson, S.J. Harris, A.J. Lough, L. Guerra, M.A. McKervey, M.J. Schwing-Weill, P. Schwinte, Selective alkali-metal cation complexation by chemically modified calixarenes. Part 4. Effect of substituent variation on the Na +/K+ selectivity in the ester series and x-ray crystal structure of the trifluoroethyl ester, J. Chem. Soc. Perkin Trans. 2 (1992) 1119–1125, https://doi.org/10.1039/p29920001119.

[23] M.A. Bernstein, S. Sýkora, C. Peng, A. Barba, C. Cobas, Optimization and automation of quantitative NMR data extraction, Anal. Chem. 85 (2013) 5778–5786, https://doi.org/10.1021/ac400411q.

[24] T. Eurolabs, EUROLABS Technical Report No. 01/2014 May 2014, EUROLAB Tech. Rep. 1/2014. (2014) 1–20. http://www.eurolab.org/documents/EUROLAB Technical Report NMR Method Development and Validation May 2014_final.pdf.

[25] G.B. Deacon, R.J. Phillips, Relationships between the carbon-oxygen stretching frequencies of carboxylato complexes and the type of carboxylate coordination, Coord. Chem. Rev. 33 (1980) 227–250, https://doi.org/10.1016/S0010-8545(00)80455-5.